Behaviour of pultruded beam-to-column joints using steel web cleats

Jawed Qureshi [a] * and J Toby Mottram [b]

[a] *School of Architecture, Computing and Engineering (ACE),University of East London*
4-6 University Way, Beckton, London E16 2RD, UK.

[b] *Civil Research Group, School of Engineering, University of Warwick, Coventry, CV4 7AL, UK.*

* Corresponding author

ABSTRACT

Response of pultruded Fibre Reinforced Polymer (FRP) beam-to-column joints with steel bolted web cleats is studied through physical testing. Two joint configurations are considered with either three or two bolts per cleat leg, as per drawings in a pultruder's Design Manual. Moment-rotation curves, failure modes and potential performance gains from semi-rigid action are determined from two batches, each having six nominally identical joints. Results show that initial joint properties for stiffness and moment can possess, at 19 to 62%, an extremely high coefficient of variation. All joints failed by fracturing within the FRP column's flange outstands. Because this failure mode has not been reported previously there is a need to establish how its existence influences joint design. As joint properties for the three- and two-bolted configurations are not significantly different, the middle (third) bolt is found to be redundant. Damage is shown to initiate within the column flange outstands when the mid-span deflection of a 5.08 m span beam, subjected to a uniformly distributed load, is span/500. This is half the serviceability vertical deflection limit recommended in the EUROCOMP Design Code and Handbook. The mean joint moment resistance for design is established to be 2.9 kNm and this is 1.5 times the moment for damage onset.

Keywords: Bolted connections; steel web cleats; pultruded joints; damage onset; moment-rotation response.

1. Introduction

Pultruded shapes of Fibre Reinforced Polymer (FRP) are used as members in pedestrian footbridges, buildings, towers, cooling towers, and walkways and platforms. Members of PFRP material are preferred [1, 2-4] because they offer significant corrosion and chemical resistance. This makes them attractive for projects where other construction materials would not satisfy the durability requirements. PFRP shapes are, moreover, chosen when electromagnetic transparency is a design requirement, as in electronics manufacturing plants [1]. They are also suitable for framed structures where either accessibility to site is limited and/or lightweight is desirable for fast deployment, such as footbridges near railway platforms.

Standard pultruded (thin-walled) FRP profiles have the same cross-sectional shape as conventional steelwork [1]. They consist of E-glass fibre reinforcement (layers of unidirectional rovings and continuous mats) in a thermoset resin based matrix. The composite material has a density about 0.25 of steel. Technical information on the pultrusion process, and PFRP shapes themselves, is given in three manufacturers' Design Manuals [2-4]. Although FRP shapes are similar to steel sections, their structural behaviour is different. Direct strengths (in the direction of pultrusion) can be over 200 N/mm^2, and this is comparable with structural grade steel. The longitudinal modulus of elasticity, at 20 to 30 kN/mm^2, is up to 10 times lower, whereas the modulus of elasticity perpendicular to the direction of pultrusion is about 0.3 of the longitudinal value [2-4]. The in-plane shear modulus has a value that is about 0.5 of the transverse modulus.

In this paper we will be concerned with construction for simple braced (non-sway) frames that have simple shear (web-cleated) connections between beams and columns, and columns and bases. To have non-sway frames diagonal bracing members are required to transfer lateral loads to the ground. Often the beams and columns are of wide flange pultruded shapes that have equal depth and flange width. As shown in Figs. 1 to 4 the method of connection with this shape is by steel bolting and joint detailing can correspond to the engineering drawings in pultruders' Design Manuals [2-4].

Presently, knowledge and understating on the response and failure of such frame joints is limited and there is lack of design guidelines too [1-5]. Because FRP material has relatively low through-thickness properties there are concerns within practice about using pultruded leg-angles for web cleat components that are assumed to offer nominally pinned joints for simple construction [5]. Previous research by Mottram [6], Mosallam [7] and Mottram and Zheng [8] provides limited joint properties from full-sized laboratory tests. These series were without specimen repetition and so there is insufficient evidence to support the proposition that pultruded cleats could be fit for purpose, because they could experience material (delamination) damage when beams are subjected to service loading.

Mottram and Zheng [9] recognised the relevance of steel cleats as connecting elements in PFRP joints. In their joint tests, that used the same test arrangement as shown in Fig. 1, the beam and column shapes were of size 203×203×9.53 mm, and from the Strongwell's standard range [3]. For joint details that were to offer semi-rigid action they chose flange cleated connections using steel angle components of 100×100×8 mm. Both major- and minor-axis tests were conducted with top and bottom steel seat cleats. There was no specimen repetition and the methods of connection were by bolting, without and with adhesive bonding. Mottram and Zheng also employed 20 mm dia. steel rods to connect opposite flange outstands of the column, with top steel seat cleats on both sides to eliminate the flexibility of the pultruded flange outstands. These internal beam-to-column joints are not known to have been adopted in practice. The only other measured properties for joints that connected pultruded members with bolted steel cleats are from Turvey [5]. With a 102×102×6.4 mm pultruded shape and stainless steel cleats of size 100×100×6 mm, Turvey characterised three joint configurations for web, flange and web, and flange only cleat details. A weakness with this work is that the end of the pultruded cantilever beam was connected to a relatively very stiff steel support angle, thereby nullifying the influence of column flange flexibility by having pultruded column flanges in the specimen configuration. By choosing a steel support, Turvey unwittingly inhibited the

mode of failure that could have occurred had the pultruded column been included in the test arrangement.

Steel or stainless steel connecting elements are adopted by fabricators because there is uncertainty on the reliability of having these key components of FRP material. In particular, leg-angle cleats cut from pultruded shapes are likely not to have acceptable fibre reinforcement to resist the joint deformations generated from prying action. Three pultruders do not provide guidelines in their Design Manuals [2-4] as to what design changes would be necessary when web cleats of steel replace those of FRP. Almost, no physical testing has been conducted when steel leg-angles are used for web cleats that form the joint detailing shown in Figs. 1 to 3. To know how safe and reliable joints with bolted steel cleats are, it is vital to characterise their moment-rotation response, modes of failure and determine the joint properties for stiffness and moment resistance.

This omission led the authors to perform a series of tests with batches of nominally identical steel web cleated joints for quantifying key joint properties. Qureshi and Mottram [10] have conducted a very similar test series with web cleats of 192 mm long, 100 mm wide and 9.53 mm thick pultruded leg-angle. The principal feature of the new contribution to understanding is that of specimen repetition. This advancement is crucial to be able to statistically quantify the joint properties, and, with confidence, to reliably establish the moment-rotation response and failure modes. Two joint configurations are characterised by way of three specimens each, with a pair of identical joints having either three- or two-bolts per cleat leg (see Fig. 2 for details). Test results are presented and discussed from the 12 major-axis joints both in terms of the two configurations and as a single population. This underpinning research gives new knowledge and insight that will aid the community when preparing design guidelines for joints in pultruded (braced, non-sway) frames.

2.   Experimental arrangement

Fig. 1 shows the test configuration in the form of two back-to-back cantilever beams with a central column. Each major-axis cruciform specimen gives two nominally identical joints, which are called the Left-side and the Right-side joint. Steel bolts and a pair of steel web cleats are used to connect beam webs to the flange outstands of the column. Qureshi and Mottram [10] and Mottram and Zheng [8-9] have used the same test configuration with connection elements of PFRP leg-angles. Turvey and Cooper [11] recognised that this is a preferred test method because it loads the beams, column and joints in a way that they could experience in a real frame. The column and beam sections are of size 254×254×9.53 mm [2], and are 1.5 m long. The shape is a wide flange section from the Pultex® SuperStructural 1525 series [2]. Steel web cleats are 192 mm long and cut from equal leg-angle of size 100×100×10 mm. A gap of 10 mm is kept between the end of the beam and the flange faces of the column to facilitate rotation of the beams. The use of web cleats together with this gap constitutes a nominally pinned joint. This type of joint is expected to transmit negligible moment across connecting components, and allows acceptable unrestrained relative rotations between framing elements.

Testing of the 12 joints is divided into two batches of six, one with three and the other with two bolts per cleat leg. The two bolted configuration is same except that the middle of the three bolts is absent. As seen in Figs 1 to 4 the bolts are placed in a line parallel to the connection shear force from the beam loading. Specimens with three bolts are denoted by label Wmj254_3M16_ST and Wmj254_2M16_ST for the two-bolted configuration. For example, Wmj254_3M16_ST defines the test joint as *W*eb-cleated with a *maj*or axis column, *254*×254×9.53 mm wide flange sections having a single row of *3 M16* bolts with *St*eel web cleats. As Fig. 1 shows the centreline of the beams is at a vertical height of 1094 mm from the base of the column. This height is controlled by the dimensions of hydraulic tension jacks and is sufficient to accommodate a downward stroke of 150 mm. To ensure both beams are subjected to same bending moments and shear forces the column section is placed on a steel rocker base fixture, having rotational freedom, as illustrated in Fig. 1.

2.1 Connection Details

Connection details shown in Fig. 2 are in accordance with Page 19-7 in the Strongwell Design Manual [3], and the minimum requirements for bolted connection geometries in the 2010 ASCE pre-standard [12]. Bolting uses standard size steel bolts of M16 grade 8.8 with 35 mm diameter by 3 mm thick steel washers. The shank bearing into FRP material (inner side of holes in beams and column) is plain to avoid any localised deformation from thread indentations. An important difference in this test series, from previous [8, 13], is that the bolt hole clearance in web of beams is kept minimal. To do this a CNC machine was used to drill holes of exactly 16 mm diameter through beam webs and connecting cleat legs. One reason that hole clearance cannot be eliminated altogether [10] is that the diameter of M16 bolts available in market ranges from 15.6 to 15.9 mm. The reason for tight-fitting holes on the beam side was to limit joint rotation due to slippage and to develop the maximum joint stiffness that could be found in the field.

The presence of bolt hole clearance leads to connection slip, and thus, slip rotation. This rotation is highly dependent on where the bolts are placed with respect to the hole. Although it has a positive effect in the form of increase in overall rotations [7-8, 13], it cannot be relied upon. In the field, bolts could be located in such a way that it might not happen. Minimising clearance on beam side also ensures that the rotation generated is predominantly due to prying action. Since having clearance holes on the column side does not influence overall rotations, a clearance of 2 mm was present for the bolt holes drilled in the column flange outstands. It also makes the assembly of the joint straightforward.

2.2 Loading procedure

Load is transferred into a beam through a hanger assembly and a 12.7 mm diameter ball bearing placed at the centre of the steel loading plate. Two hydraulic tension jacks apply the point load. The load applied in this manner ensures vertical loading. The general test arrangement is shown in Fig. 3. Load is applied at a distance of 1.016 m from centreline of the column. This distance is governed by

anchor points on the strong floor having spacing of 408 mm centres. The applied load on the Left and Right sides is measured via two tension load cells having capacity of 9 kN with a resolution of ±0.01 kN. Two manual hydraulic pumps are used to operate the jacks. The rocker base fixture ensures equal load increments to the beams.

Joint moment is established by the vertical load times the lever arm distance of 1016 mm taken from the loading point to the centreline of the column member. The reason for taking moment from centreline of the column, rather than the plane separating the column flange and web cleats to loading point is that the column web panel constitutes part of the joint. Eurocode 3 Part 1-8 [14] provides a clear description of what a joint is. It defines the joint to be the zone where two or more members are attached together. Concerning the test configuration in Figure 1 the beam-to-column joint consists of all the material (e.g. beam and column web and columns flange outstands) and connection components (i.e. bolting and web cleats) that lie between the pair of clinometers measuring the joint rotation.

The specimen is loaded under load control in 0.25 kN increments. A time interval of five minutes is maintained between two increments to make visual inspection and to take measurements. Readings are taken immediately after load is applied and five minutes later. This procedure allows onset and progressive material damage to be observed. Load is continuously increased until the joint rotation increases significantly without noticeable change in the moment or it is deemed that specimen instability might occur. Each specimen is unloaded and reloaded at overall joint rotations of 20 and 30 mrad to record permanent rotations. The specimens are unloaded at the end of the testing and final permanent rotation noted. Further details on the test method are given in Qureshi and Mottram [10]. To ensure connecting elements in the joint are in firm contact, bolts are tightened to snug-tight condition. This condition is achieved when bolts will not turn any further after full effort of a worker using an ordinary spud wrench.

2.3   Instrumentation

Typical instrumentation to measure joint properties is shown in Fig. 4. Rotations of beams are measured by clinometers C1 and C3, placed at a distance of 130 mm from the end of the beam adjacent to the column flange. Column rotation is measured by C2, and the difference between beam and column rotations give the Left and Right joint rotations. The 'secondary' rotation due to relative connection slippage between a beam's web and the pair of cleats is determined, using the geometric relationship in Qureshi and Mottram [10], via displacements from the four transducers LTL, LBL, LTR and LBR. The positions of these transducers are seen in Fig. 4. The displacements are measured to a resolution of ± 0.01 mm and the rotation to 0.02 mrad (linear to $\pm 1\%$ over a 10° range).

Qureshi and Mottram [10] confirmed that the joints with PFRP web cleats fail by delamination, which is seen first at the top of cleats and near the fillet radii [7, 8]. With steel web cleats, the pultruded members are likely to fail because cleats are no longer the weakest link. This is because steel has yield strength (275 N/mm^2) that is many times higher than the through-thickness tensile strength of the FRP and a modulus of elasticity 10 to 20 times higher. Steel cleats will have a much higher resistance to the low level of prying action. As a result the tension force (at top bolt level) from the prying action causes the column flange outstands to undergo significant flexural deformation. To monitor this joint deformation, which was not noticeable when equivalent cleats were PFRP [10], the horizontal distance between the outer surfaces of the column flanges at the level of the top and bottom bolts is measured. This result is given by $h_{\mathrm{prying}} - h$, where h is the undeformed depth (see Fig. 2) and h_{prying} is the deformed depth (refer to Fig. 5). The measurements are taken by means of a vernier calliper at each load increment, and at the start and end of the test.

3.   Results and discussion

Tables 1 and 2 present joint properties for the two batches of specimens having three- and two-bolted joint configurations. The slip rotation is deducted from the overall rotation of the joints in these tables. Therefore, the properties reported are due to the effect of the prying action alone. Minimum

and maximum values for a particular column are highlighted using bold font. Specimen labels are given in column (1), which also identify if the joint is on the Left or Right side. For the linear moment-rotation response the initial joint properties are given in columns (2) to (4). They are the initial moment (M_i), initial joint rotation (ϕ_i) and initial joint stiffness S_i ($= M_i/\phi_i$). Similarly, the equivalent properties for onset of damage, which has a specific definition introduced later, are given in columns (5) to (7) by M_j, ϕ_j and ($S_j = M_j/\phi_j$). Columns (8) to (9) give the maximum moment (M_{max}) and maximum rotation (ϕ_{max}). At the bottom of Tables 1 and 2 the mean and coefficient of variation (CV) of each joint property are presented.

3.1   Joint Properties

Prior to giving a discussion on damage onset, the initial and maximum test results will be discussed. For the Wmj254_3M16_ST batch, the moment-rotation remains linear up to a mean M_i of 0.92 kNm. The minimum and maximum initial moments in column (2) of Table 1 are 0.68 and 1.27 kNm, and the six joints give a relatively high coefficient of variation (CV) of 29%. Initial rotation (ϕ_i) is also highly variable with test results ranging from 0.7 to 4.1 mrad. The mean rotation of 2.3 mrad has a very high CV of 62%. Due to the high variation in these initial properties the initial joint stiffness has a CV of 47%. From column (4) of Table 1 the mean, minimum and maximum S_is are 502, 302 and 913 kNm/rad. From the data in columns (8) and (9) it is observed that M_{max} and ϕ_{max} do not change significantly for the Wmj254_3M16_ST batch; and these properties have the relatively low CVs of 1.4% and 13%. The mean M_{max} is 3.4 kNm and the mean ϕ_{max} of 52 mrad.

From the Wmj254_2M16_ST batch the moment-rotation response is found to be linear to a mean initial moment of 0.73 kNm. M_i in column (2) of Table 2 ranges from 0.56 to 0.87 kNm, giving a CV of 19%. The corresponding mean initial rotation in column (3) is 1.4 mrad, minimum and maximum ϕ_is are found to be 0.8 and 2.2 mrad. Initial joint rotational stiffness (S_i) has a mean of 577 kNm/rad

and a CV of 38%. This is similar to the Wmj254_3M16_ST batch results in column (4) of Table 1, and shows a large variation in initial joint properties. From Table 2 the mean M_{max} is 3.82 kNm and mean ϕ_{max} is 64 mrad. As with the three bolted joint case, it is noteworthy that the maximum joint properties in columns (8) and (9) do not vary much, giving relatively small CVs of 3.5% and 6%. Comparison of Table 1 and 2 suggests that the joint properties of two- and three-bolted configuration are not much different with marginally higher maximum moment and rotation in former case. This finding shows that the third bolt is not needed to resist the effect of the beam loading. This slight increase in the joint properties is by no means an indication of better performance of two- compared with three-bolted configuration. The maximum joint properties depend on when the test was stopped, which again relies on either instability or ultimate failure of the specimen under consideration.

3.2   Damage onset

It is not straightforward with steel web cleats to precisely define the joint rotation (ϕ_j) for damage onset. With similar cleating of FRP, Qureshi and Mottram [10] found that damage initiated as delamination cracking was easily seen by the human eye at the top of pultruded cleats. With steel cleats failure occurs within the web-flange junction of the column. For this failure mode damage onset is defined as the point on the moment-rotation curve when audible noises, emanating from inside the column flanges, were first heard. Additional evidence for this stage establishing damage is that the M-ϕ response was noticeably non-linear and the column flanges were experiencing a significant outward flexural deformation, in line with the top bolt level.

Fig. 5 shows the extent of this flange deformation (h_{prying} (TOP) – h (TOP)) and (h_{prying} (BOTTOM) – h (BOTTOM)) when ϕ in test Wmj254_3M16_ST1.2 had reached 50 mrad. All specimens failed by cracking in web-flange junction of the column near top bolt level and progressed downwards to bottom bolt level. Due to prying action, column flange outstands deflect outwards at the top bolt level and there was no change in the section's depth at the bottom bolt level. It is found that the steel cleats did not noticeably deform or have yielding. To establish the extent of permanent damage, one of the

failed columns was sectioned, just above the middle bolt level. On one side of the web, the flange outstands were cut off to expose the extent of internal damage in the form of delamination cracks. As Fig. 6 shows there is fracturing in the region of the web-flange junction and significant delamination in the flanges. The presence of these internal damage highlights that the stiffness of the column will have continually reduced as PFRP damage progressed. It is this progressive deterioration that helps to explain the non-linear M-ϕ response, such as seen by the test curves in Figs. 8 and 9. At the end of a test the internal fracturing was seen to reach the top free end of column, which is 280 mm from the top flange of the beams.

Plotted in Fig. 7 are the changes in column depth, h_{prying}, at the centreline of the TOP and BOTTOM bolt levels. The increase in depth with increasing M at TOP is given by the solid line and that at the BOTTOM by the dashed line (which shows it to be virtually constant and nearly equal to h, until M is 3 kNm). After M exceeds 3 kNm the TOP h_{prying} is seen to increase very rapidly, from 3% to 8% of h. This suggests that the joint is close to ultimate failure.

3.3   Moment-rotation curves

Plotted in Figs 8 and 9 are the moment-rotation (M-ϕ) curves for specimens Wmj254_3M16_ST1.3 and Wmj254_2M16_ST1.2, these are typical of batch results. Joint rotation due to connection slip has been deducted from the measured joint rotation. The solid line is for the joint that is on the Left-side and the dashed line for its paired joint, on the Right-side. The solid circular symbols show the moment and rotation at damage onset using the definition introduced in Section 3.2. The unloading and loading cycles, when the overall joint rotation reaches approximately 20 and 30 mrad, are also presented in the plots. Through careful preparation of the members and cleats, slip rotation was successfully minimised, if not eliminated completely. The amount of slip rotation was less than 0.5 mrad at damage onset and did not increase thereafter.

The saw-tooth shape to the M-ϕ curves in Figs 8 and 9 is the result of taking readings straight after a load increment was applied, and 5 minutes later. The change shows the extent of relaxation in this short period of time due to damage progression. The more noticeable drop in moment, after M exceeds 2.5 kNm, does suggest that the Left and Right joints are now experiencing significant material damage. To further support this behaviour, the moment reduction becomes more prominent as the Left and Right joint rotations approach their ϕ_{max}.

Although both M-ϕ curves in Fig. 8 remain linear up to a moment of 0.70 kNm the value of S_i (from Table 1) on the Left side, at 913 kNm/rad, is twice that for the Right side, at 444 kNm/rad. A physical explanation for this considerable difference cannot be given. It is noted that because both M_i and ϕ_i are at the low end of their measurement scales this could be a contributing factor. The extent of permanent deformation for Wmj254_3M16_ST1.3 can be observed from the loading and unloading cycles presented in Fig. 8. For the first unloading stage at 20 mrad there was a permanent rotation in both joints of 5 mrad. On reloading to the same M, the Right side rotated to 33 mrad and, because there was less deterioration, the Left joint's rotation was 25 mrad. This suggests reloading causes further material degradation inside the column flanges, and it was now impractical to maintain 'identical' joint rotations on both sides. The specimen was, again, unloaded and reloaded with the results that the permanent rotations were 6 and 11 mrad on Left and Right sides. No obvious peak moment was established and further loading was stopped when joint deformation was deemed to be excessive; termination of additional loading stages therefore gave the readings in columns (8) and (9) of Table 1 for M_{max} and ϕ_{max}.

Fig. 9 gives the equivalent M-ϕ characteristics for Wmj254_2M16_ST1.2, again, after taking into account secondary slip rotation. The response of this two-bolt configuration is found to be similar to three-bolted situation. Wmj254_2M16_ST1.2 has a linear M-ϕ to a moment (M_i) of 0.56 kNm. This is followed by a non-linear response that is directly linked to outward flexural deformation of the

column flanges adjacent to the centrelines of the top bolts. S_i from column (4) in Table 2 is 744 and 386 kNm/rad for the Left and Right joints. Because the Right side has nearly twice the stiffness, this specimen show, again, that a steel web cleated joint can possess an initial rotational stiffness much higher than that on the other side. The mean moment at damage onset is about 2 kNm for both two- and three-bolted configurations. Once material damage is known to exist the properties presented in Table 2 give significantly lower variation. As an example, S_js for Wmj254_2M16_ST1.2 are 271 and 239 kNm/rad, a difference of 13% compared to 92% (from S_i when response starts to go non-linear). For the two-bolt specimen in Fig. 9 it was found that there was a 9% increase (23 mm) in column depth ($h_{prying} - h$) at M_{max} near top bolt level.

From the results of 12 joints the mean M_j is 2 kNm and the mean M_{max} is 3.6 kNm. From these moments it is observed that onset of damage has occurred when joint moment is about 55% of the maximum moment. This percentage difference in terms of M_{max} was found by Qureshi and Mottram [10] in their series of joint tests with pultruded cleats. Note that M_{max} with steel cleats was twice that resisted by the PFRP cleats, and that the latter cleat material gave a mean M_j of only 1.0 kNm. One finding from the two test series is that damage occurs, by delamination fracturing either in the cleats, when they are pultruded, or in the column flanges, when cleats are of steel, at a moment (M_j) that is half of M_{max}.

3.4   Design moment resistance

For design of framed structures the moment resistance of the joints has to be known. According to American standard AISC 360-10 [15], this moment resistance is the maximum moment that the joint is capable of carrying. The steel standard states that the moment resistance can be determined either from a physical test or from analysis using an Ultimate Limit State model. As seen by the M-ϕ curves in Figs 8 and 9 the joints with steel web cleats did not exhibit a clear maximum moment. M keeps on increasing, until a test was stopped. In the absence of an obvious peak moment, standard AISC 360-10 [15] recommends taking the moment resistance to be the moment at a rotation of 20 mrad.

Applying this approach the mean joint moment resistance, for use in design, is found to be 2.9 kNm. Pultrex® SuperStructural wide flange shapes have a flexural strength of 300 N/mm^2 [2] and the major-axis second moment of area (I) is 8.34x10^7 mm^4 for the 254×254×9.53 mm section. Using conventional engineering beam theory the moment resistance of the section to (linear elastic) rupture is 198 kNm, which is > 60 times the joints' mean moment resistance (2.9 kNm).

3.5   Failure when cleats are of steel

The extent of flexure in the column flange outstands is shown in Figs 10(a) to 10(c). Fig. 10(a) indicates the localised nature of this column deformation. With respect to a steel ruler, pressed against the undeformed flange below the bottom bolt level, Fig. 10(b) shows the degree of deformation for the geometric test property h_{prying}. Because the steel cleats possess relatively high strength and stiffness, their deformation from transmitting moment and shear force is not discernable. Owing to the layered construction of pultruded material, cleats of FRP are susceptible to delamination failure caused by prying where tensile stresses in the through-thickness direction are highest [10]. As this study shows when steel replaces pultruded FRP, joint failure is shifted from the web cleating [10] into the column. At M_{max} the flanges deflected outwards resulting in 20 to 24 mm increase in overall depth of the column at top bolt level. This can be seen in Fig. 10(c) and this localised column deformation represents an 8 to 9% increase in overall column depth.

Manufacturers of pultruded shapes do offer some guidance for beam members having PFRP web-cleated joints [2-4]. Strength information for the web-cleated joints is reported, but not for the moment resistance. It is based on the three modes of failures being, bearing of cleat material near fastener holes, or shear failure at the heel of the angle, or shear failure in bolting [1]. None of these failure modes were observed with either FRP [10] or steel cleats in the test series presented in this paper. Given that there are no specific guidelines for steel cleats there is a need for a revision of the Design Manuals [2-4] to account for the actual modes of failure and how they affect joint performance.

3.6 Serviceability and performance gain due to semi-rigid action

In order to take advantage of semi-rigid action the joint has to possess sufficient end rotation prior to onset of material damage, as this could detrimentally affect structural integrity during the structure's service life. Applying the damage criterion introduced earlier in this paper the mean ϕ_j, from column (6) of Tables 1 and 2, is 7.7 mrad, having a CV of 9.8% and standard deviation of 0.75 mrad. Hence, using the expression of Mean - 1.82 × SD (Annex D of [16]) the characteristic rotation at damage onset is 6.3 mrad. For a simply supported beam subjected to a Uniformly Distributed Load (UDL) this characteristic damage rotation of 6.3 mrad equates to a mid-span deflection of span/500. Note that in the EUROCOMP Design Code and Handbook [17] the recommended vertical deflection limit is span/250 for a Serviceability Limit State.

Semi-rigid action may be utilised in the design of PFRP beams to achieve a performance gain. Turvey [18] developed closed-form expressions to calculate the response of a 'semi-rigid' beam, with respect to the identical simply supported beam, by means of performance indices. These indices are for the reduction in beam deflection, the increase in load-carrying capacity and/or the increase in span for the same deflection. The use of these equations requires knowledge of the rotational stiffness of the semi-rigid joints and its variation. Because S_i from Tables 1 and 2 is unreliable for the reason already discussed, this stiffness measure cannot be used. Although Turvey [18] recommends using S_i with his formulae, the authors advocate that the rotational stiffness should be the secant value at damage onset. This is because S_i exhibits a too high CV (41% for joints in this study) and cannot be reliably used. The S_js in Tables 1 and 2 are more reliable; especially since the batch of 12 joints have a CV of 10%.

To evaluate the performance gain, from $S_j >$ zero, let us assume the beam is shear rigid and subjected to a uniformly distributed load. Fig. 11 presents a plot to show the potential benefit obtained from the semi-rigid action. The abscissa scale is for span-to-depth ratios from 0 to 40, and the ordinate is for

the load enhancement index (λ_Q) which represents the additional load for a specified mid-span deflection limit. A step-by-step procedure to calculate λ_Q for a span-to-depth ratio of 20 is given in the Appendix. The plot in Fig. 11 shows that λ_Q increases with more load gained as the span-to-depth ratio increases. For example, exploiting the mean S_j (266 kNm/rad) from Tables 1 and 2, for the steel web cleat details in Fig. 2, leads to a load increase of 22% and 42% for the span-to-depth ratios of 20 and 40, respectively. Owing to the linear elastic and small displacement assumption in the analytical treatment [18], the load enhancement (λ_Q) and deflection reduction (λ_δ) indices are inversely proportional to each other. This means there will be reductions of 0.82 and 0.70 to the mid-span deflection at these two span-to-depth ratios. This preliminary evaluation demonstrates that either a reduction in mid-span deflection or an increase in UDL is practical if the rotational stiffness of practical joint details is accounted for. The initial or secant joint rotational stiffness under service loading can be favourably exploited to achieve performance gains in terms of deflection reduction, or load or span enhancement.

4.   Concluding remarks

Beam-to-column joints for Pultruded Fibre Reinforced Polymer (PFRP) members with bolted steel web cleats for a nominally pinned joint are characterised through testing two batches of six nominally identical joints. One batch had three bolts per cleat leg and the second had the middle bolt of the three removed. Because test results showed that there is no significant difference between two batches, the authors recommend that the third (middle) bolt detailing can be removed from the engineering drawing in the Strongwell Design Manual [3].

For the preparation of design guidelines the following key findings from an evaluation of the test results are of relevance:

- It is found that by having web cleats of steel the onset of damage will occur within the pultruded FRP column flange outstands. Such FRP failure is initiated by prying action causing considerable flexural deformation of the column flange outstands. None of the Design Manuals [2-4] report this type of failure. Owing to the field application of steel cleats in PFRP frames there is a need to include this type of failure mode and its design implications when revising the manuals.

- To characterise the 'stiffest' joint in practice, the specimens were fabricated with tight-fitting bolt holes between the pair of steel cleat legs and the web in a beam member. Because 'off-the-shelf' M16 steel bolts have a shank diameter of 15.6 to 15.9 mm the joint rotation due to connection slip between cleats and beam was not entirely eliminated. Its magnitude was found to be only 0.5 mrad at damage onset, and it did not increase significantly thereafter. All rotation results presented are compensated for slip rotation to ensure that the rotation at damage onset is its lowest possible field value.

- The linear region on the moment-rotation curves is relatively small and non-linearity in joints' response is found when rotation is more than 4 mrad. All initial moment, rotation and stiffness values show variability with coefficients of variation of 28%, 62% and 41%, respectively, with stiffnesses (ranging from 302 to 913 kNm/rad) based on combined results from 12 joints. It is found that the unreliability of these initial joint properties means they cannot be used to adequately represent the joints in real frames.

- Taking the characteristic value of joint rotation at damage onset as 6.3 mrad, it has been shown that (delamination) damage could occur within the column member when the mid-span deflection of a beam with a uniformly distributed load is span/500. This is half the serviceability vertical deflection limit recommended in the EUROCOMP Design Code and Handbook [17]. The rotation at damage onset is likely to increase (but not guaranteed) when bolting has clearance holes of 1 mm [4] or larger [2-3].

- By using Turvey's [18] closed form equations with the joint rotational stiffness at damage onset a performance gain of 22% is identified in terms of the increase in load carrying

capacity of a shear rigid pultruded beam having a uniformly distributed load and a span-to-depth ratio of 20. This load increase is relative to the deflection of the same beam being simply supported. Load enhancement will increase with increasing span-to-depth ratio, and *vice versa*.

- When a joint test does not show a clear peak moment in the moment-rotation response, AISC 360-10 [15] specifies that the value corresponding to a rotation of 20 mrad should be used. For the purpose of design the mean moment resistance from the 12 joints is 2.9 kNm. This moment is 1.5 times the moment at damage onset (2 kNm), and only 1.5% of the section moment of resistance (198 kNm) when flexural strength of the Pultrex® SuperStrucutral pultruded shape is taken to be 300 MPa [2].

Acknowledgements

Appendix for calculation of load enhancement index (λ_Q)

Load enhancement index (λ_Q) is calculated according to the procedure given in Turvey [18]. We shall consider a beam with a uniformly distributed load. In order to calculate the load enhancement index (λ_Q) the deflection reduction index (λ_δ) has first to be determined from:

$$\lambda_\delta = \left(\frac{1 + k_2 \beta}{k_4 + k_2 \beta} \right) \qquad\qquad \text{A.1}$$

where

k_2 From Table 1 [18] is 10.

k_4 From Table 1 [18] is 5.

β Dimensionless rotational flexibility of the beam end connection given by ($E_L I / KL$), where

         E_L Longitudinal modulus of elasticity for pultruded beam (is 27.6 kN/mm^2 from Creative Pultrusion Design Manual [2])

         I Major-axis second moment of area of beam cross-section (is 8.34x10^7 mm^4 from Creative Pultrusion Design Manual [2])

         K Rotational stiffness of the beam end connection [18] (is $S_j = 266$ kNm/rad from the mean joint rotational stiffness from the 12 joints in Tables 1 and 2)

         L Beam span is 5080 mm (based on a span-to-depth ratio of 20 for 254×254×9.53 shape).

λ_Q is calculated from the inverse of Equ. (A.1):

$$\lambda_Q = \frac{1}{\lambda_\delta} \qquad (A.2)$$

Assuming the PFRP beam is shear-rigid, β, λ_δ (A.1) and λ_Q (A.2) are calculated to be:

$$\beta = \left(\frac{E_L I}{KL}\right) = \left(\frac{27.6 \times 1000 \times 8.34 \times 10^7}{266 \times 10^6 \times 5080}\right) = 1.7$$

$$\lambda_\delta = \left(\frac{1 + k_2 \beta}{k_4 + k_2 \beta}\right) = \left(\frac{1 + 10 \times 1.7}{5 + 10 \times 1.7}\right) = 0.82$$

$$\lambda_Q = \frac{1}{\lambda_\delta} = \frac{1}{0.82} = 1.22$$

References

[1]   Bank LC. Composites for construction - Structural design with FRP materials. John Wiley & Sons, New Jersey, 2006.

[2]   Anonymous. The new and improved Pultex® pultrusion design manual. Creative Pultrusions Inc., Alum Bank, PA. (www.creativepultrusions.com/library.html) (April 2, 2012).

[3]   Anonymous. Strongwell design manual. Strongwell, Bristol, VA. (www.strongwell.com/) (April 2, 2012).

[4]   Anonymous. Fiberline design manual for structural profiles in composite materials. Fiberline Composites A/S, Kolding, Denmark. (www.fiberline.com/read-more-about-fiberline-online-tools) (April 2, 2012).

[5]   Turvey GJ. Moment–rotation tests on bolted end connections in pultruded GRP beams-tests with stainless steel cleats and an assessment of their performance relative to GRP cleats. In: Proceedings of the Ninth European Conference on Composite Materials (ECCM 9: From Fundamentals to Exploitation), Brighton, 4-7 June 2000.

[6]   Mottram JT. Connection tests for pultruded frames. Research Report CE47, Civil Engineering Group, School of Engineering, University of Warwick, Coventry, U.K, 1994.

[7]   Mosallam AS. State-of-the-art on connections for pultruded frame structures. In: Connecting with Pultrusion, Proceedings of the Fourth EPTA World Pultrusion Conference, European Pultrusion Technology Association, Harderwijk, The Netherlands, 1998.

[8]   Mottram JT, Zheng Y. Further tests on beam-to-column connections for pultruded frames: Web-cleated. J Compos Constr 1999;3(1):3-11.

[9]   Mottram JT, Zheng Y. Further tests on beam-to-column connections for pultruded frames: Flange-cleated. J Compos Constr 1999;3(3):108–116.

[10]   Qureshi J, Mottram JT. Moment-rotation response of nominally pinned beam-to-column joints for frames of pultruded fibre reinforced polymer. Eng Struct 2012 (under review).

[11]   Turvey GJ, Cooper C. Review of tests on bolted joints between pultruded GRP profiles. P I Civil Eng-Str B 2004;157(3):211-233.

[12]   Pre-standard for Load and Resistance Factor Design (LRFD) of pultruded Fiber Reinforced Polymer (FRP) structures (Final). American Composites Manufacturers Association, American Society of Civil Engineers, November 9, 2010.

[13]   Mottram JT. Nominally pinned connections for pultruded frames. In Clarke JL editor. Structural Design of Polymer Composites - EUROCOMP Design Code and Handbook, S. & F. N. Spon, London, 1996. p.703-718.

[14]   BS EN 1993-1-8:2005. Eurocode 3: Design of steel structures - Part 1-8: Design of joints. British Standards Institution, United Kingdom, 2005.

[15]   AISC 360-10. Specification for Structural Steel Buildings. American Institute of Steel Construction. Chicago, Illinois, USA, June 22, 2010.

[16]   BS EN 1990:2002. Eurocode 0 - Basis of structural design. British Standards Institution, United Kingdom, 2002.

[17]   Clarke JL (Editor). Structural design of polymer composites - EUROCOMP design code and handbook. E. & F.N. Spon, London, 1996.

[18]   Turvey GJ. Analysis of pultruded GRP beams with semi-rigid end connections. Compos Struct 1997;38(4):3-16.

Table 1. Joint properties for beam-to-column joint test Wmj254_3M16_ST (compensated for slip)

Specimen label (1)	M_i (kNm) (2)	ϕ_i (mrad) (3)	$S_i = M_i/\phi_i$ (kNm/rad) (4)	M_j (kNm) (5)	ϕ_j (mrad) (6)	$S_j = M_j/\phi_j$ (kNm/rad) (7)	M_{max} (kNm) (8)	ϕ_{max} (mrad) (9)
Wmj254_3M16_ST1.1 (Left)	1.25	4.1	**302**	1.97	7.3	271	3.42	50
Wmj254_3M16_ST1.1 (Right)	1.27	4.0	316	1.99	7.7	**258**	3.44	**59**
Wmj254_3M16_ST1.2 (Left)	0.80	1.2	649	2.04	6.4	316	3.43	51
Wmj254_3M16_ST1.2 (Right)	0.83	2.2	386	2.06	7.7	268	3.44	55
Wmj254_3M16_ST1.3 (Left)	0.68	0.7	**913**	2.02	**6.4**	**318**	3.34	**40**
Wmj254_3M16_ST1.3 (Right)	0.71	1.6	444	2.04	**7.9**	259	3.35	57
Mean of 6	0.92	2.3	502	2.02	7.2	282	3.40	52
CV	29%	62%	47%	1.7%	9.2%	9.9%	1.4%	13%

Table 2. Joint properties for beam-to-column joint test Wmj254_2M16_ST (compensated for slip)

Specimen label (1)	M_i (kNm) (2)	ϕ_i (mrad) (3)	$S_i = M_i/\phi_i$ (kNm/rad) (4)	M_j (kNm) (5)	ϕ_j (mrad) (6)	$S_j = M_j/\phi_j$ (kNm/rad) (7)	M_{max} (kNm) (8)	ϕ_{max} (mrad) (9)
Wmj254_2M16_ST1.1 (Left)	0.76	0.8	**896**	1.92	7.6	254	3.74	**59**
Wmj254_2M16_ST1.1 (Right)	0.75	1.9	398	2.15	8.5	252	3.71	61
Wmj254_2M16_ST1.2 (Left)	0.56	0.8	744	2.03	**7.5**	**271**	3.98	64
Wmj254_2M16_ST1.2 (Right)	0.56	1.4	**386**	2.03	8.5	239	4.00	68
Wmj254_2M16_ST1.3 (Left)	0.86	1.3	646	2.03	8.0	254	3.74	62
Wmj254_2M16_ST1.3 (Right)	0.87	2.2	393	2.03	**8.8**	**231**	3.74	**69**
Mean of 6	0.73	1.4	577	2.03	8.2	250	3.82	64
CV	19%	41%	38%	3.5%	6.7%	5.5%	3.5%	6%
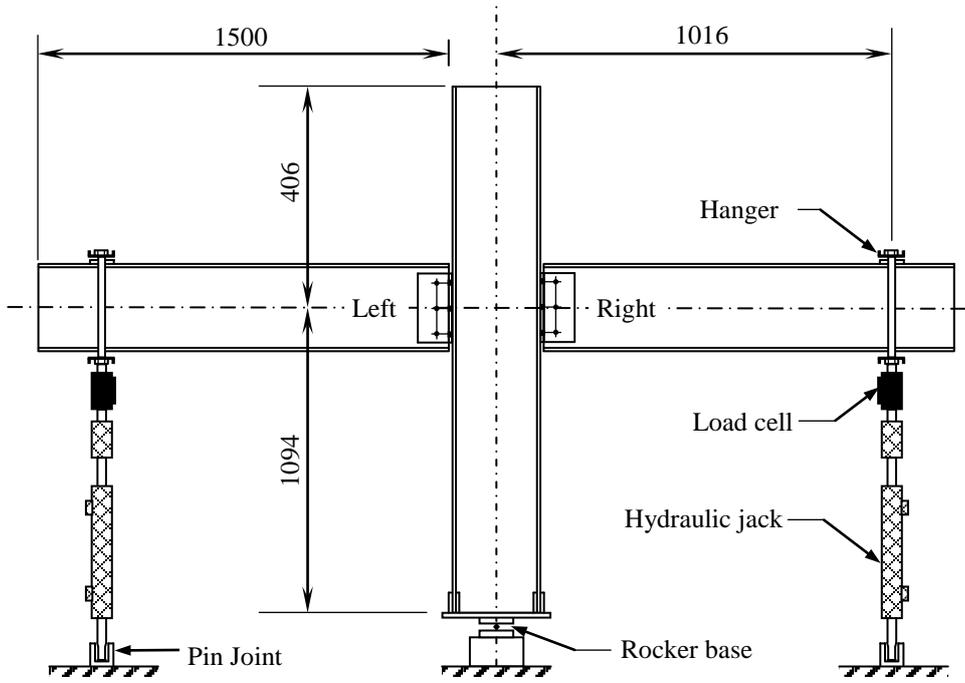
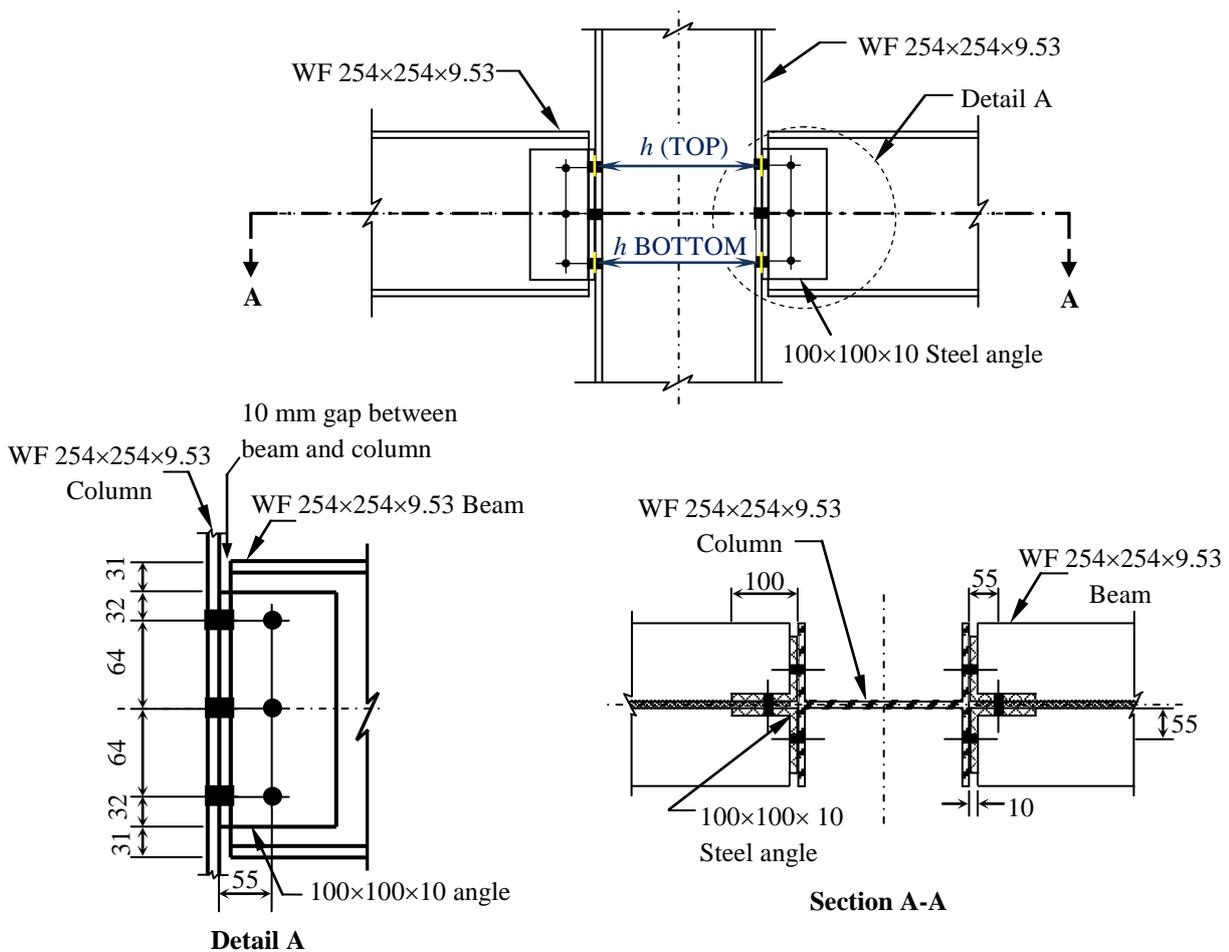Fig. 1. Cruciform test configuration and loading arrangement.

Fig. 2. Connection details for beam-to-column joint tests with structural steel cleats (All dimensions are in mm).
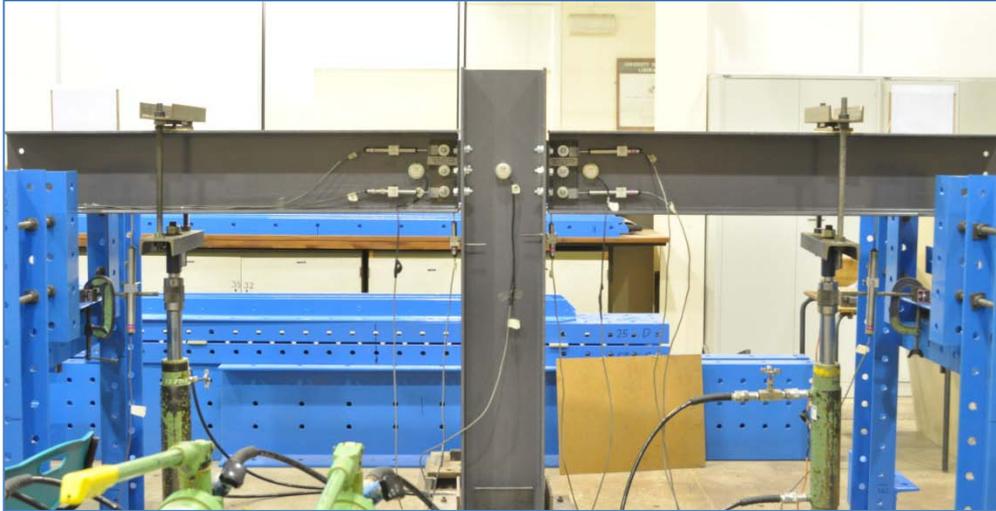
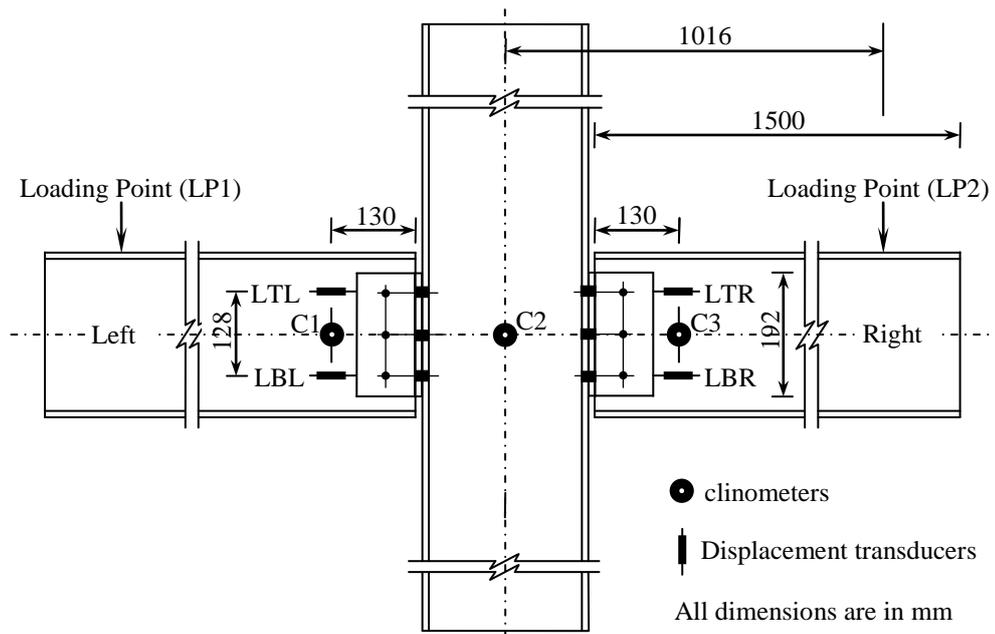Fig. 3. General test arrangement for the steel web cleated beam-to-column joint tests.

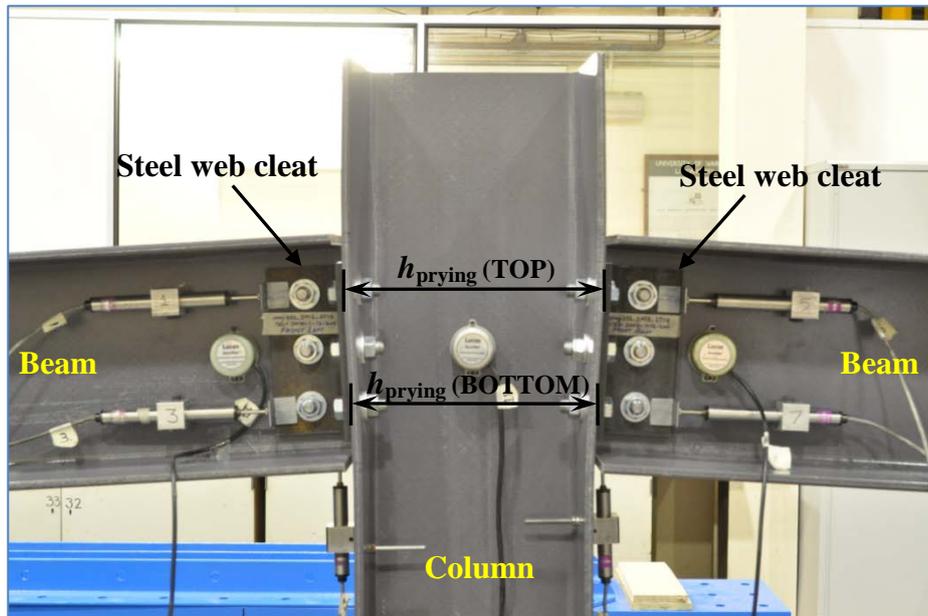Fig. 4. Location of instrumentation for the steel web cleated beam-to-column joint tests.

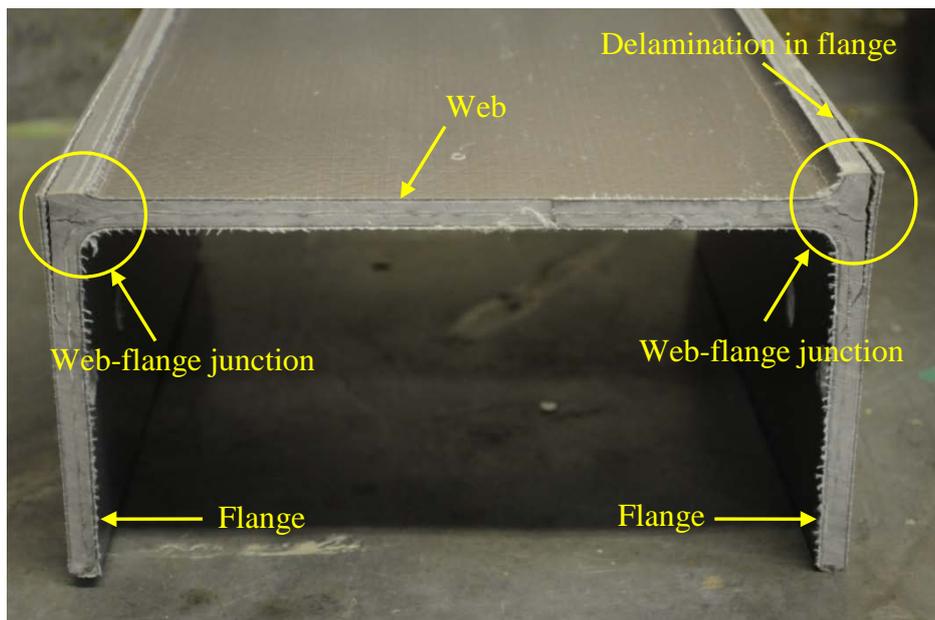Fig. 5. Close-up of Left and Right joints in Wmj254_3M16_ST1.2 when M_{max} is applied.

Fig.6. Internal fracture pattern in column section (cut above middle bolt hole level).
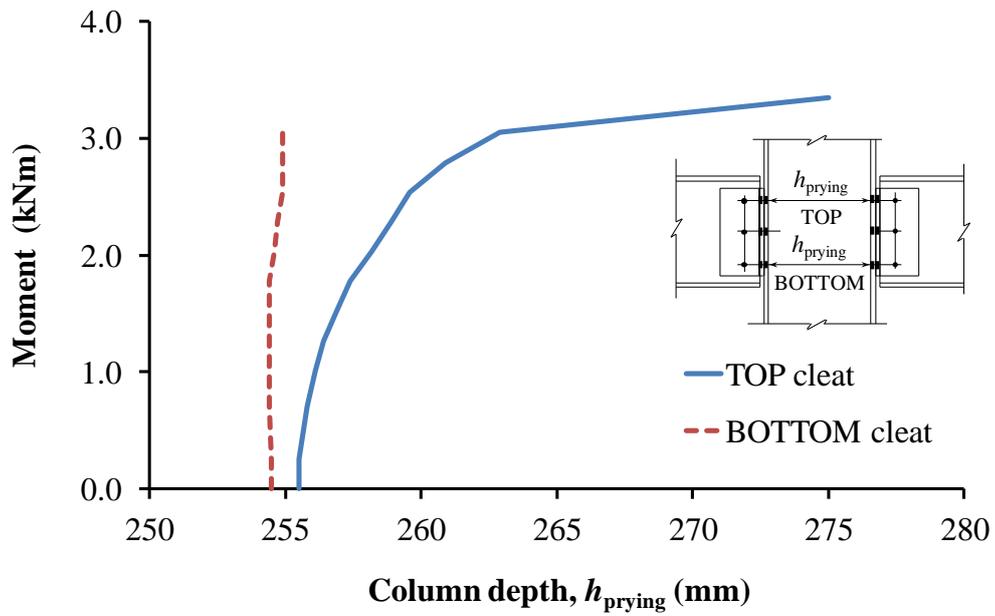
Fig. 7. Column depth (h_{pyring}) versus joint moment for Wmj254_3M16_ST1.3.
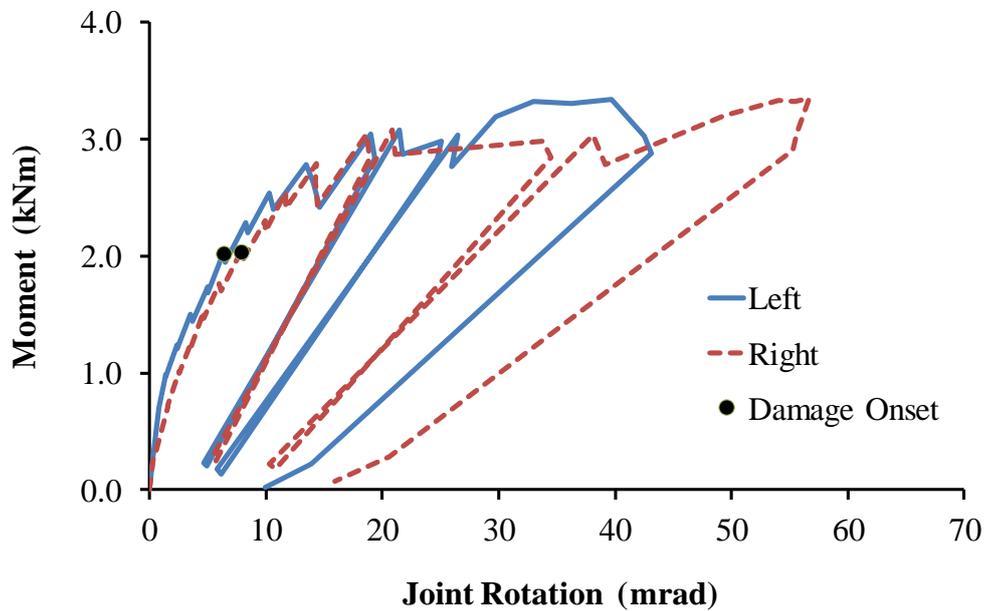
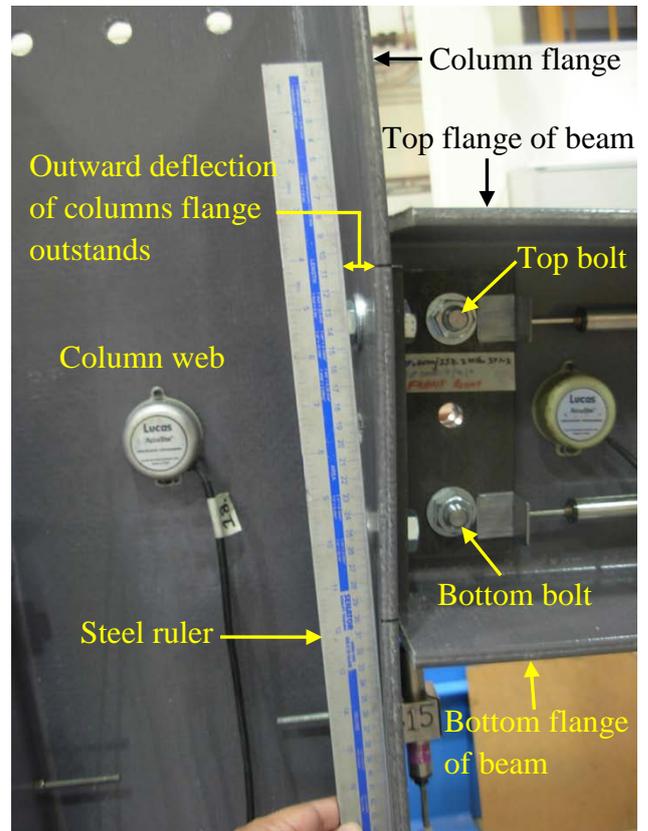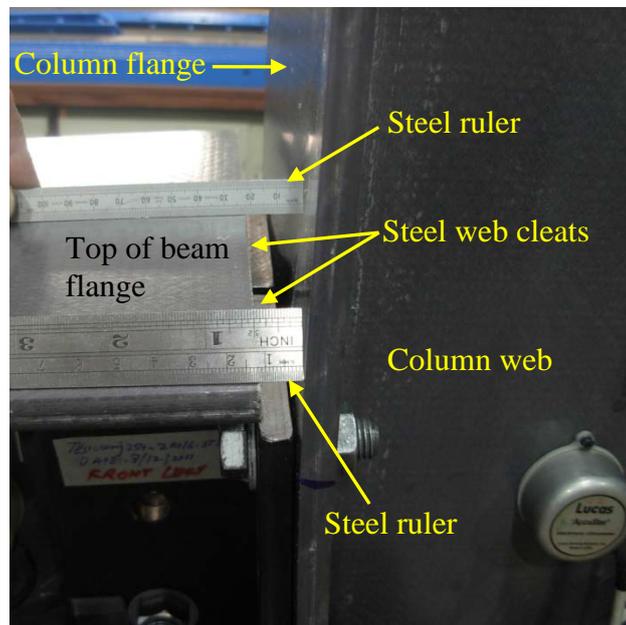Fig. 8. Moment-rotation curves for specimen Wmj254_3M16_ST1.3 (compensated for slip).
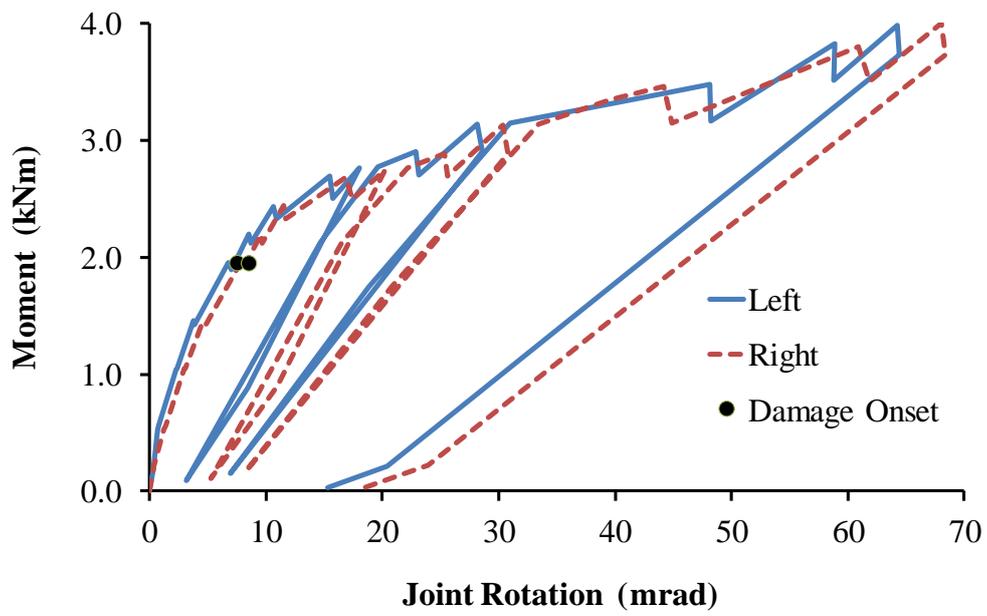
Fig. 9. Moment-rotation curves for specimen Wmj254_2M16_ST1.2 (compensated for slip).
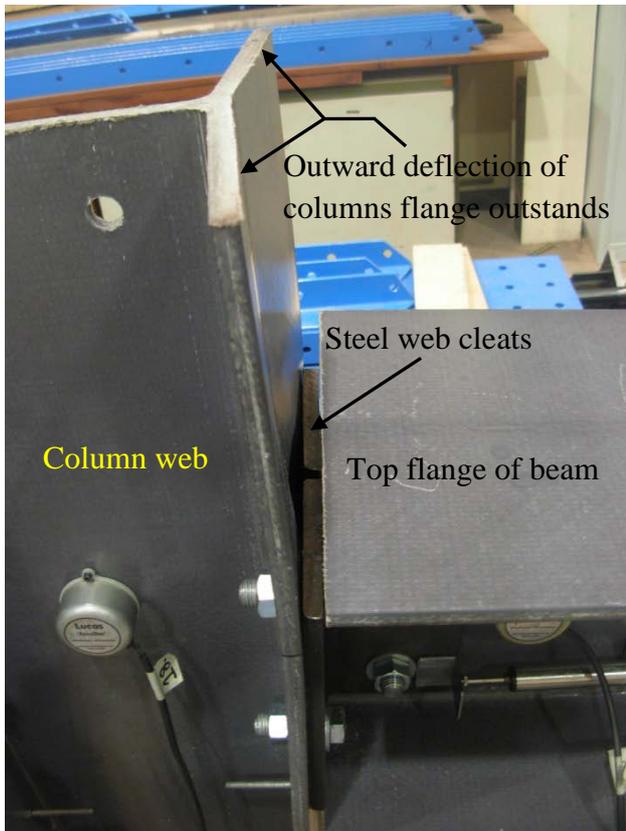
Fig. 10. Different views of localised column deformations when joints had failed: (a) Outward flexure of column flanges; (b) Flexure of column flanges with respect to a vertically placed ruler; (c) Extent of column deformation for ϕ_{max}.
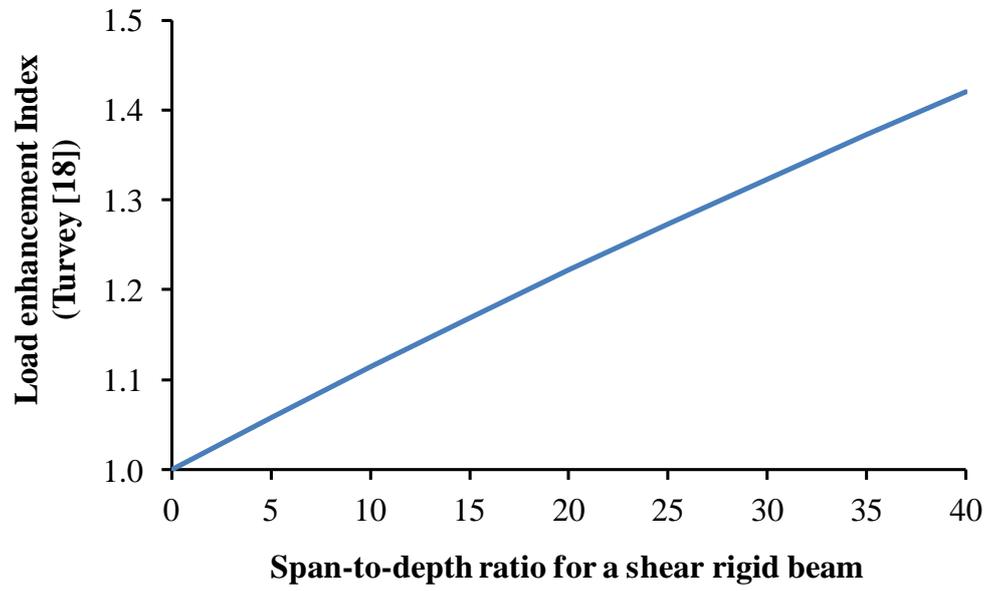
Fig.11. Load enhancement index (λ_Q) versus span-to-depth ratio for shear rigid pultruded beams with semi-rigid end connections (steel web cleats).